DOI: https://doi.org/10.15407/rpra30.04.250
UDC 621.396.965
PACS 02.70.–c, 05.40.Ca, 06.20.Dk, 07.05.Tp, 84.40.–x

Yu.F. Logvinov, Yu.O. Pedenko, O.V. Bukin
O.Ya. Usikov Institute for Radiophysics and Electronics of the NAS of Ukraine
12, Acad. Proskury St., Kharkiv, 61085, Ukraine
E-mail: yuriy.pedenko@gmail.com

OFF-AXIS TARGET ILLUMINATION IN RADAR OVER-SEA TRACKING USING AN ACTIVE PHASED ARRAY ANTENNA

Subject and Purpose. *This paper addresses the challenge of measuring the angular coordinates of over-sea low-altitude targets and strives to improve the measurement accuracy of radar systems that employ high-resolution algorithms implemented through active phased array antennas (APAAs). The primary purpose is to substantiate the effectiveness of off-axis target illumination in the context of sea clutter and multipath. Off-axis target illumination reduces the depth of the probing-signal interference fading over the radar-to-target path. The investigated illumination method focuses on mitigating errors in target angle measurements by multi-channel methods based on high-resolution algorithms, such as root-MUSIC. One of the main spoilers of measurement accuracy when using those algorithms is the noise in the radar receiving channels. Off-axis target illumination helps avoid a deep fade of the signal, thereby enhancing the signal-to-noise ratio (SNR) in the receiving channels of APAA-equipped radar systems, which contributes to target tracking stability despite destructive multipath interference.*

Methods and Methodology. *The study employs computer simulations within a multipath radio-wave propagation model for a rough sea surface, allowing for both specular and diffuse reflections. The power distribution of diffuse reflections and their mapping along the propagation path are evaluated using the empirical glistening-surface model, the most advanced to date.*

Results. *Quantitative assessments of the effectiveness of off-axis target illumination have been obtained in the context of fading conditions produced by multipath radio wave propagation over the sea surface. The optimal illumination angles have been identified. They help avoid deep fades over a wide range of sea states. These optimal angles are confined within 0.6 to 0.75 of the beamwidth of the radiation pattern. The lower end of the indicated range refers to the diffuse sea clutter, and the upper end corresponds to the specular reflection of the probing signal. In the most adverse cases, a gain in the SNR reaches 6…8 dB.*

Conclusions. *It has been confirmed that off-axis illumination allows decreasing the depth of the illumination signal fades, which ensures more stable target tracking by angular coordinates. Recommendations for selecting off-axis illumination angles have been formulated.*

Key words: *illumination level, off-axis illumination, active phased array antenna (APAA), low-altitude target, rough sea surface, multipath propagation, elevation angle, antenna pattern, computer modeling.*

Introduction

A current challenge for modern multichannel radar systems is enhancing the angle measurement accuracy for airborne objects tracked in the near-surface region above a disturbed sea. One promising approach to addressing this issue involves high-resolution methods implemented using antenna arrays.

In our previous works, we emphasized the effectiveness of elevation-angle estimation algorithms, particu-

Citation: Logvinov, Yu.F., Pedenko, Yu.A., Bukin, O.V., 2025. Off-axis target illumination in radar over-sea tracking using an active phased array antenna. *Radio Phys. Radio Astron.*, **30**(4), pp. 250–257. https://doi.org/10.15407/rpra30.04.250

larly root-MUSIC [1] and Matrix Pencil [2], which significantly mitigate the effects of multipath interference. According to research results in [3], the employment of these algorithms significantly reduces measurement errors within the elevation range 0.2—0.25 to $2\Theta_{0.5}$, where $\Theta_{0.5}$ is the half-power beamwidth of the antenna pattern synthesized by the array aperture.

However, despite their high robustness to multipath interference, the indicated methods may fall short in estimation accuracy under elevated levels of internal noise in the radar receiving channels [3]. To guarantee measurement accuracy, maintaining a sufficient signal-to-noise ratio (SNR) is essential. In this study, the SNR is defined as the direct signal power received at each channel input from the target and related to the internal noise power at those inputs. For a pinpoint isotropic retransmitting target, the SNR is assumed to be the same in all receiving channels.

In active radars, one possible way to boost performance is to increase the target illumination level. This paper examines one implementation of this approach, which does not require increasing the probing signal power but improves reception energy conditions by adjusting the illumination geometry.

1. Off-axis illumination under multipath propagation

The amplitude of the received direct signal bounced off a flying target is determined by the target illumination power and is proportional to the magnitude of the vector sum of the amplitudes of the direct probing signal and its sea clutter multipaths. Depending on the phase relationships of these components, which change as the target moves away from the radar and are additionally affected by the sea state and sea clutter, the illumination level has fluctuations, and so do the signal-to-noise ratios (SNRs) at the inputs of the reception channels.

The most critical situation arises from negative interference between direct and specular signals. In this case, the resultant signal amplitude drops significantly. This not only makes accurate angular coordinate measurements more difficult but also reduces the likelihood of target detection. To address these issues, various methods have been proposed in the literature, a brief overview can be found in [4]. In particular, the likelihood of interference-induced fading can be reduced by using multiple operating frequencies [5] or by adjusting radar antenna heights [6]. Another known approach involves increasing the received signal level by switching the probing signal polarization, which helps maximize the radar cross-section of the target [7].

However, implementing the aforementioned methods in multichannel APAA-based radars poses significant technological challenges. To name a few, it is essential to achieve high-precision matching of the phase-amplitude and polarization characteristics of the channels across wide frequency ranges. Or high-speed responsivity is required from the control system to detect and track maneuverable or fast-moving targets.

Understandably, there is a pressing request for simpler instrument solutions. The current work is based on the off-axis target tracking approach previously proposed [8] for monopulse radars. In it, once the target drops below a specified elevation angle, the antenna system gets fixed in a steady position, and the elevation angle is estimated when an error signal appears.. This mode allows reducing wavefront phase distortions caused by specular returns in the "target–radar" segment, thereby reducing the angle measurement error.

Contemporary high-resolution systems generally manage the task of accurate angular tracking even in environments with multipath interference. Off-axis illumination is mainly important as a practical way to enhance target illumination when negative interference occurs in the "radar–target" segment. To assess the effectiveness of this approach, the present study aims to gather quantitative characteristics of the off-axis method under typical conditions, implying different sea states, various target altitudes above the sea surface, and elevation angles smaller than the antenna pattern beamwidth, where the application of high angular-resolution algorithms is particularly appropriate.

2. Initial conditions and research methodology

The present study uses computer simulation. A vertical linear phased array antenna with equidistant transmit-receive modules can be considered as an APAA. This is acceptable because:

- direct and specular signals illuminating the target propagate in the same elevation plane that passes

through the vertical axis of the active phased array, while diffuse reflections extend beyond it quite subtly [9];

• the radiation patterns of one-dimensional and two-dimensional arrays coincide in that plane when the used aperture weighting functions are identical.

This simplifies the modeling process with no loss of generality.

A rectangular aperture weighting function is used in the modeling. It best matches an APAA of a rectangular shape because it provides the highest radiation power when all active elements operate at their maxima. It also creates the steepest slopes in the active phased-array pattern, which helps increase the level of illumination on a target by suppressing sea clutter.

The effectiveness of off-axis target illumination is evaluated by comparing illumination levels with those produced by the direct target illumination.

The evaluation parameters are:

• operating wavelength λ is 3.2 cm;

• APAA vertical size is 2.5 m;

• half-power beamwidth $\Theta_{0.5}$ of the synthesized transmitting antenna is 0.65°;

• APAA centre height h_a above the mean sea level is 25 m;

• target heights h_t above the mean sea level are 5, 10, and 15 m;

• target elevation ε ranges from 0.25 to $0.75\Theta_{0.5}$;

• for the target elevation ε interval 0.25 to $0.75\Theta_{0.5}$, target distances D are 590 to 1760 m at a 5 m target height, 1170 to 3500 m at a 10 m height, and 1760 to 5200 m at a 15 m height;

• root mean square σ_h of wave heights is 0.065 m (sea states 1—2), 0.12 m (state 2), 0.21 m (states 2—3), 0.32 m (states 3—4), and 0.54 m (states 4—5) [10].

As the considered problem concerns the radio wave propagation near the sea surface at grazing angles much smaller than the Brewster angle, it is safe to assume that for both vertical and horizontal polarizations, the sea clutter coefficient is nearly unity in the undisturbed sea case, and the reflection phase is close to 180°.

According to Vvedensky's formula, the path difference between the direct and specular rays is $\Delta \approx 2h_a h_t / D$ and becomes $\Delta \approx 2h_a\varepsilon$ as $\varepsilon \approx h_t / D$. Since $h_a = \text{const}$ in this study, one should bear in mind that the same-type interference extrema on all the considered paths will correspond, with sufficient accuracy, to the same elevation angles of the target. The path geometry used in the study is shown in Fig. 1.

Because randomness is imposed on the illumination levels by the sea swell, their comparisons are made based upon distribution quantiles at orders 0.01 and 0.001. Each distance quantile is calculated using a sufficiently large number of independent realizations of the illumination signal field.

Formulas (1) and (2) below determine each random field intensity $\dot{E}$ as follows,

$$\dot{E}(D) = \\ = \sum_{n=1}^{N} \dot{E}_n(D) G_n \exp\{-jkr_n \sin[\beta(D) - \varepsilon(D)]\}, \quad (1)$$

where $\dot{E}_n$ is the field intensity that the n-th APAA element creates at the target location; $N = 156$ is the number of APAA elements; $k = 2\pi/\lambda$ is the wave number; $r_n = d(n - (N+1)/2)$ is the n-th APAA element displacement from the APAA centre; $d = \lambda/2$ is the distance between adjacent APAA elements; G_n is the value of the aperture weighting function at the n-th APAA element; ε and β are, respectively, the elevation angles of the target and the main lobe axis of the synthesized radiation pattern, both measured relative to the direction toward the "effective horizon", defined as the bisector of the angle formed by the directions to the target and target specular image. For off-axis illumination, $\beta(D) = \text{const}$. For direct illumination, $\beta(D) = \varepsilon(D)$.

The field intensity created at the target location by the n-th APAA element was calculated as:

$$\dot{E}_n(D) = \dot{E}_n^{(dir)}(D) + \dot{E}_n^{(spec)}(D) + \sum_{s=1}^{S} \dot{E}_{s,n}^{(diff)}(D), \quad (2)$$

where S is the number of diffusely reflecting adjacent segments obtained by dividing the "glistening surface" along the propagation path; s is the index of the segment; $\dot{E}_n^{(dir)}$, $\dot{E}_n^{(spec)}$, $\dot{E}_{s,n}^{(diff)}$ are the total field intensity components produced by the n-th APAA element, corresponding, respectively, to the direct ray, the specular return, and the ray from the s-th segment. The calculation of these signals was performed using the methodology developed by the authors in [11] and based on the "glistening surface" theory [9, 12].

The study proceeds through four stages. First, signal field realizations are computed using equa-

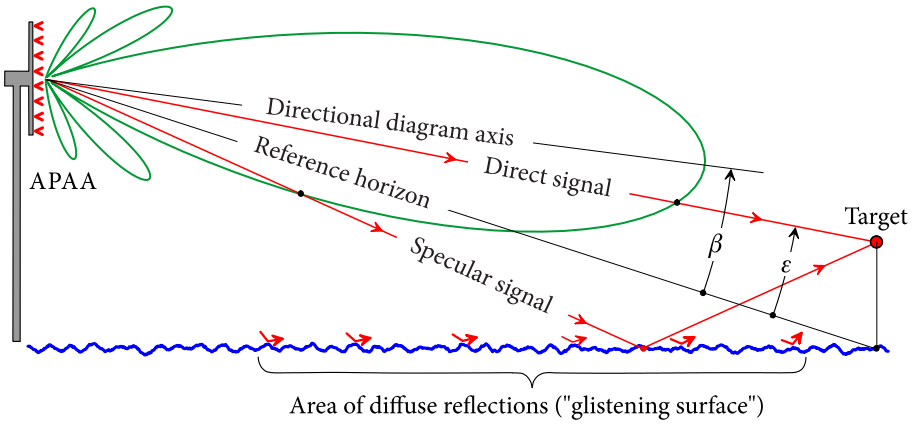

Fig. 1. The path geometry

tion (2) for a selected sequence of distances. The spacing between them is chosen to capture detailed, distance-dependent illumination-level variations caused by the interference between the direct and reflected signals. At each sea state and various APAA and target height combinations, a sequence of operations is carried out as follows:

1. The initial distance D is specified.

2. The instant coefficients, ρ_s and ρ_d, of specular and diffuse reflection are calculated based on the instant distance D, root mean square σ_h of wave heights, APAA height h_a, and target height h_t above the sea level.

3. The $\dot{E}_n^{(dir)}$ and $\dot{E}_n^{(spec)}$ data arrays are computed.

4. Given a specified maximum slope of 0.05 radians of sea surface irregularities, the boundaries of the "glistening surface" participating in diffuse reflection are identified. This glistening surface over the propagation path is divided into approximately 30 m-long diffusely reflective segments.

5. Each segment is assigned to random local diffuse-reflection parameters, including: the reflection point locations (equiprobable along the segment) and the reflection coefficient with quadrature components obeying the normal distribution. Based on the local parameters of the segments, an $\dot{E}_{s,n}^{(diff)}$ array is calculated for the current realization of local segment parameters.

6. Using equation (2), the realizations of the field intensity $\dot{E}_n(D)$ created at the target location by each of the N elements of the APAA are computed.

7. Steps 5 and 6 are repeated until the specified number of independent realizations at the current distance is reached. In the considered case, their number was 50 thousand.

8. The next distance D is taken, and steps 2 to 7 are repeated until the whole set of distances is processed.

The first-stage realizations of the signal field $\dot{E}_n(D)$ are stored in a database and will be used later in the calculations at various target illumination angles. This reduces computational effort and improves the comparison of the results at different angles.

At the second stage, formula (1) is used to calculate the target illumination level versus distance and for different illumination angles β. To implement off-axis illumination, the β values were selected from the range ε to $0.9\Theta_{0.5}$ and taken as a sequence of $0.05\Theta_{0.5}$ increments to achieve the strongest target illumination at the critical points, i.e., in the field minima vicinities. Meanwhile, distance dependences for direct target illumination were also calculated at the same initial data.

In the subsequent presentation, the illumination levels are expressed relative to the free-space illumination level $\dot{E}_0(D) = \sum_{n=1}^{N} \dot{E}_n^{(dir)}(D) G_n$, with the normalized values in the form $E^*(D) = \overline{\dot{E}(D)} \Big/ \overline{\dot{E}_0(D)}$.

The third stage renders statistical processing of the normalized values to obtain quantiles that bound the domains of their most probable values. Of use are the quantile pairs $Q_{0.01} - Q_{0.99}$ and $Q_{0.001} - Q_{0.999}$.

At the fourth stage, an analysis is conducted on the distance dependences of the lower illumination-level bounds at different off-axis angles, addressing the two tasks:

1. The optimal off-axis illumination angle is determined for each scenario studied. To do this, from each group of dependences at fixed sea state and target height but different illumination angles, the one

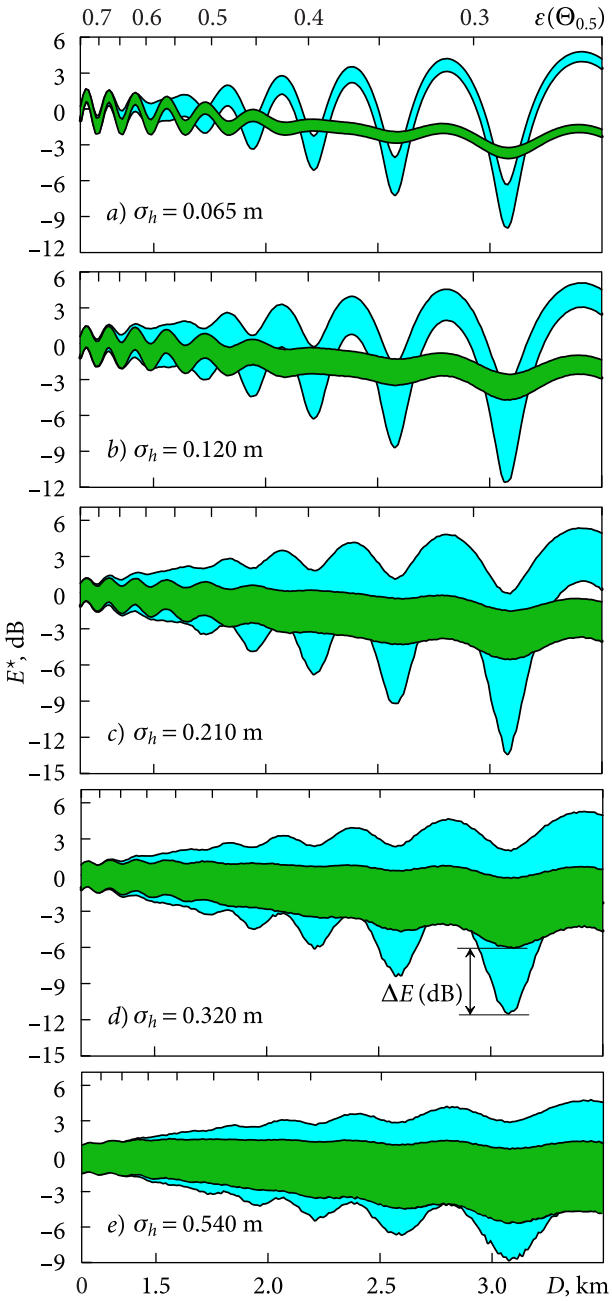

Fig. 2. Distance dependences of the levels of illumination on a 10 m high target at different sea states

Table 1. **Direct illumination levels at the field minimum under different sea states**

σ_h (m)	ρ_s	ρ_d	E^* (dB)
0.065	0.95	0.06	–9.9
0.120	0.86	0.15	–11.6
0.210	0.65	0.30	–13.4
0.320	0.40	0.39	–11.2
0.540	0.21	0.40	–8.9

whose lower boundary of the field interference minima is the highest is chosen.

2. The gain in off-axis target illumination at the field interference minima is determined relative to the direct illumination level.

3. Discussion of the research results

Figure 2 presents target illumination levels versus distance for a 10 m target height. These levels are shown as shaded areas bounded above by the quantile $Q_{0.999}$ and below by the quantile $Q_{0.001}$. The light and dark grey plots indicate, respectively, direct illumination and off-axis illumination at optimal angles. The plots were obtained for σ_h values ranging from 0.065 to 0.54 m. The distance dependences of the coefficients ρ_s and ρ_d under the same conditions are seen in Fig. 3.

The levels of direct target illumination are characterized by periodic fluctuations that increase with the distance to the target and are driven by two factors: on the one hand, the specular reflection coefficient increases, and on the other, the angular separation between the target and its mirror image decreases. The first factor stems from the grazing angle decrease at the specular reflection point. The second is associated with the specular image direction movement to the APAA pattern maximum, where the slope in elevation angle is the flattest. As a result, the antenna gain coefficients in the target and its mirror image directions converge, leading to deeper signal fading.

Notice that the deepest fading occurs in the sea-state transitional region specified by the changeover from specular to diffuse reflection. This is evident from Tab. 1, which lists the illumination levels corresponding to the field minimum at a 3.1 km range ($\varepsilon = 0.28\Theta_{0.5}$) under different sea state conditions. The deepest fading is observed at sea state 2—3 ($\sigma_h = 0.21$ m).

In contrast to direct illumination, the off-axis method is applied in an area where the antenna pattern is characterized by a steep slope and away from the main lobe maximum. Consequently, at the field minima, the difference between the direct and reflected signals increases, which underlies the effectiveness of the off-axis illumination. The price to pay is the decrease in illumination level at the field maxima, but it is considered a low priority in the current task context.

The key evidence for applying the off-axis method is the $\Delta E = \Delta E^{*}$ gain increase against direct target illumination. To determine it, use Fig. 2, *d* as a guide. Having processed the simulation results covering the initial conditions listed above, we conclude that off-axis illumination is effective within an elevation angle range of approximately 0.5 to $0.6\Theta_{0.5}$. Furthermore, the farther the target moves on, the lower the target elevation angle, and the better the off-axis illumination effectiveness. This is crucial for maintaining a sufficient signal-to-noise ratio as the target recedes.

The gain in target illumination at optimal angles is viewed in Fig. 4 for a 10 m high target. The plots in Figs. 4, *a* and *b* were obtained by comparing the 0.01 quantiles and the 0.001 quantiles, respectively. Each curve is constructed by five points corresponding to the illumination minima within the elevation angle range 0.25 to $0.5\Theta_{0.5}$. Importantly, the outcomes for the 5 and 15 m high targets are identical to those of the 10 m high target issues in Fig. 4, providing very similar quantitative and qualitative characteristics.

Let us examine the outcomes related to optimal illumination angles. In selecting optimal angles, priority was given to the gain in target illumination at the far-field interference minimum corresponding to the elevation angle $\varepsilon = 0.28\Theta_{0.5}$, which, as previously noted, was consistent across all target heights. The optimal illumination angles are listed in Tabl. 2.

As seen from Tab. 2, in situations characterized by relatively strong specular reflection, the optimal angle is $0.75\Theta_{0.5}$. This value nearly coincides with a deviation of $0.748\Theta_{0.5}$ from the main lobe peak, where the slope of the pattern main lobe is maximum.

Additionally, according to Tabl. 2, as the sea surface roughness and, correspondingly, diffuse reflection increase, the optimal off-axis angle decreases to $0.6\Theta_{0.5}$. To interpret this effect, take up a hypothe-

Table 2. **Optimal off-axis angles β as fractions of the main lobe width $\Theta_{0.5}$**

σ_h (m)	h_t (m)		
	5	10	15
0.065	0.75	0.75	0.75
0.120	0.75	0.75	0.75
0.210	0.70	0.75	0.75
0.320	0.60	0.70	0.75
0.540	0.60	0.65	0.70

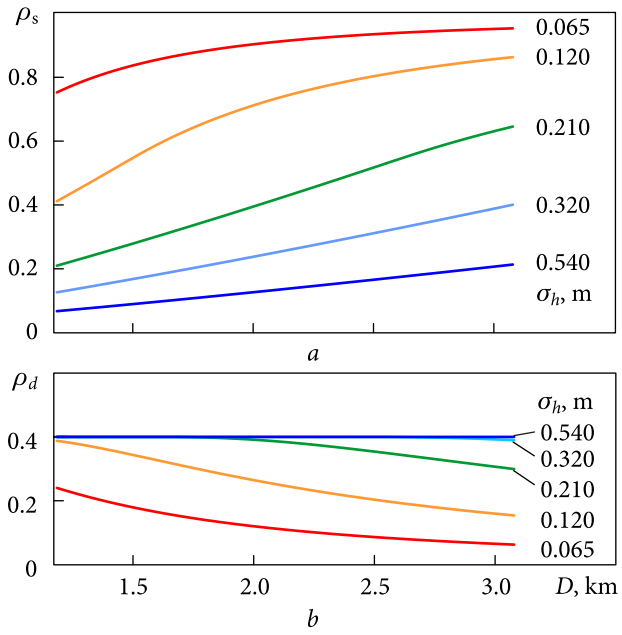

Fig. 3. Distance dependences of the specular and diffuse reflection coefficients at different sea states

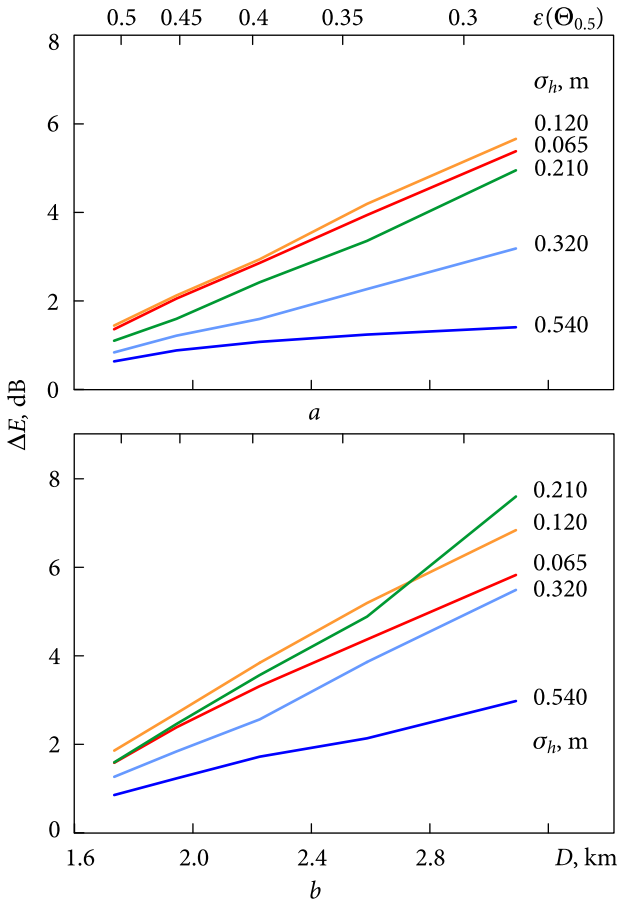

Fig. 4. The gain in target illumination at field minima under different sea states: *a* — comparing the 0.01 quantiles and *b* — comparing the 0.001quantiles

tical scenario, assuming that there is no specular reflection, and the diffuse reflection along the whole path is at a maximum, the reflection coefficient being $\rho_d = 0.4$. In this case, the optimal illumination angle is $0.6\Theta_{0.5}$. The same optimal illumination angle values were obtained for the target height $h_t = 5$ m and wave height $\sigma_h \geq 0.32$ m (see Tab. 2), i.e., nearly in the context of hypothetical case conditions. Indeed, in these situations, the reflection coefficient values in the vicinity of the far-field minimum ($D = 1.55$ км and $\varepsilon = 0.28\Theta_{0.5}$) are as follows:

- for $\sigma_h = 0.32$ m: $\rho_s = 0.21$ and $\rho_d = 0.4$;
- for $\sigma_h = 0.54$ m: $\rho_s = 0.11$ and $\rho_d = 0.4$.

This closeness is attributed to that the grazing angles ψ_s and, hence, the sea surface roughness parameters are significantly larger at $h_t = 5$ m than at $h_t = 10$ m, and the more so at $h_t = 15$ m. And that the grazing angle $\psi_s \approx (h_a + h_t)/D$ with $h_a >> h_t$ is larger than at the other target heights is caused by shorter ranges at the same elevation angles.

Conclusions

A method of off-axis target illumination has been proposed and investigated for low-altitude over-sea target tracking by radar systems possessing ultra-high angular resolution implemented using active phased array antennas (APAAs). The purpose of this method is to mitigate interference-induced deep fades in illumination and thus improve the coordinate measurement accuracy under multipath radio wave propagation conditions.

The core idea of the method is to deflect upward the axis of the illumination beam pattern by an angle of $0.6—0.75\Theta_{0.5}$ relative to the reference horizon, which is defined as the bisector between the directions to the target and target specular image. This mitigates the detrimental effect of sea-swell multipaths on the level of low-altitude target illumination. In response, the angle-of-arrival measurement errors are smaller, and the signal-to-noise ratio at the inputs of the radar receiving channels increases.

It has been established that the effectiveness of off-axis illumination begins to show when the target descends below $0.5—0.6\Theta_{0.5}$ and increases as the elevation angle decreases, reaching its peak in target tracking at marginally low altitudes. Thus, at elevation angles of about $0.25—0.3\Theta_{0.5}$, the signal-to-noise ratio at the inputs of the radar receiving channels gains 6…8 dB compared to direct target illumination.

REFERENCES

1. Rao, B.D., Hari, K.V.S., 1989. Performance *analysis of Root-MUSIC. IEEE Trans. Acoust. Speech Signal Process.*, **37**(12), pp. 1939—1949. DOI: 10.1109/29.45540
2. Sarkar, T.K., Pereira, O., 1995. Using the matrix pencil method to estimate the parameters of a sum of complex exponentials. *IEEE Antennas Propag. Mag.*, **37**(1), pp. 48—550. DOI: 10.1109/74.370583
3. Logvinov, Yu.F., Pedenko, Yu.O., Reznichenko, M.G., 2024. On the achievable upper limit of the elevation angles of effective direction finding of targets over the sea by the root-MUSIC method provided with adequate a priori parameters. *Radio Phys. Radio Astron.*, **29**(4), pp. 281—292 (in Ukrainian). DOI: 10.15407/rpra29.04.281
4. Yang, Yong, Yang, Boyu, 2024. Overview of radar detection methods for low altitude targets in marine environments. *J. Syst. Eng. Electron.*, **35**(1), pp. 1—13. DOI: 10.23919/JSEE.2024.000026
5. Yunhe, Cao, Shenghua, Wang, Yu, Wang, Shenghua, Zhou, 2015. Target detection for low angle radar based on multi-frequency order-statistics. *J. Syst. Eng. Electron.*, **26**(2), pp. 267—273. DOI: 10.1109/JSEE.2015.00032
6. Yang, Yong, Wang, Xue-Song, 2023. Enhanced Radar Detection in the Presence of Specular Reflection Using a Single Transmitting Antenna and Three Receiving Antennas. *Remote Sens.*, **15**(12), pp. 3204—3214. DOI: 10.3390/rs15123204
7. Quoc, An Nguyen, 2017. On a solution to improve the object detection ability of radars by dynamic polarization method. *ASEAN Journal on Science and Technology for Development (AJSTD)*, **23**(1), 4. DOI: 10.29037/ajstd.97
8. Dax, P.R., 1976. Keep Track of that Low-Flying Attack. *Microwaves*, **15**(4), pp. 36—38, 40, 41.
9. Barton, D.K., 1974. Low-Angle Tracking. *Proc. IEEE*, 62(1), pp. 687—704. DOI: 10.1109/PROC.1974.9509
10. Barton, D.K., Ward H.R., 1984. *Handbook of Radar Measurement*. Artech House Publishers.
11. Razskazovskiy, V.B., Pedenko, Yu.A., 2003. A model for millimeter- and centimeter-waves field over a sea surface designs for investigation the methods for low-flying targets elevation angle measurement. In: V.M. Yakovenko, ed. 2003. *Radiofizika i elektronika*. Kharkov: IRE NAS of Ukraine Publ. **8**(1), pp. 22—33.
12. Beckman, P., and Spizzichino, A., 1963. *The scattering of electromagnetic waves from rough surfaces*. London: Pergamon Press.

Received 15.06.2025

Ю.Ф. Логвінов, Ю.О. Педенко, О.В. Букін
Інститут радіофізики та електроніки ім. О.Я. Усикова НАН України
вул. Акад. Проскури, 12, м. Харків, 61085, Україна

ПОЗАОСЬОВЕ ОПРОМІНЕННЯ ЦІЛІ ПІД ЧАС РАДІОЛОКАЦІЙНОГО СУПРОВОДУ НАД МОРЕМ З ВИКОРИСТАННЯМ АКТИВНОЇ ФАЗОВАНОЇ АНТЕННОЇ РЕШІТКИ

Предмет і мета роботи. Роботу присвячено проблемі підвищення точності вимірювання кутових координат маловисотних цілей над морем у РЛС, що використовують алгоритми високої роздільності, реалізовані на основі активних фазованих антенних решіток (АФАР). Основна мета дослідження — обґрунтування ефективності позаосьового опромінення цілі в умовах багатопроменевого відбиття радіохвиль від поверхні моря, що дозволяє зменшити глибину інтерференційних завмирань зондуючого сигналу на ділянці поширення від РЛС до цілі. Досліджуваний спосіб опромінення спрямований на зниження похибок у вимірюванні кутових координат цілі при використанні багатоканальних методів, заснованих на алгоритмах високої роздільності, зокрема root-MUSIC. Для таких алгоритмів шуми приймальних каналів РЛС є однією з головних причин зниження точності. Позаосьове опромінення дозволяє уникнути глибоких завмирань сигналу, тим самим підвищуючи співвідношення сигнал/шум (SNR, від англ. *signal-to-noise ratio*) у приймальних каналах РЛС з АФАР, що сприяє стабільному супроводу цілі в умовах несприятливої інтерференції багатопроменевих сигналів.

Методи та методологія. Дослідження виконано з використанням комп'ютерного моделювання. В експериментах застосовувалася модель багатопроменевого поширення радіохвиль над збуреною морською поверхнею, яка враховує як дзеркальне, так і дифузне відбиття. Розподіл потужності дифузного відбиття та його положення вздовж траси розраховувалися відповідно до емпіричної моделі «блискучої поверхні», яка на сьогодні вважається найбільш досконалою.

Результати. Отримано кількісні оцінки ефективності позаосьового опромінення цілі в умовах завмирань, викликаних багатопроменевим поширенням радіохвиль над морем. Визначено оптимальні кути опромінення, які дозволяють уникнути глибоких завмирань у широкому діапазоні станів морської поверхні. Їхні значення перебувають у діапазоні 0.60…0.75 від ширини діаграми направленості випромінювання. При цьому нижня межа діапазону відповідає дифузному відбиттю зондуючого сигналу від збуреної поверхні моря, а верхня — дзеркальному. Збільшення SNR у найбільш несприятливих випадках досягає 6…8 дБ.

Висновки. Результати дослідження підтверджують можливість використання позаосьового опромінення для зменшення глибини завмирання зондуючого сигналу, що забезпечує більш стабільний супровід цілі за кутовими координатами. Сформульовано рекомендації щодо вибору кутів позаосьового опромінення.

Ключові слова: *рівень опромінення, позаосьове опромінення, активна фазована антенна решітка (АФАР), маловисотна ціль, збурена поверхня моря, багатопроменеве поширення, кут місця, діаграма направленості, комп'ютерне моделювання.*